PROTEINS: Structure, Function, and Genetics 37:576–581 (1999)

Graphical Method for Force Analysis: Macromolecular Mechanics With Atomic Force Microscopy

Hong Qian[1]* and Bruce E. Shapiro[2]
[1]*Departments of Applied Mathematics and Bioengineering, University of Washington, Seattle, Washington*
[2]*Department of Biomathematics, University of California School of Medicine, Los Angeles, California*

ABSTRACT **We present a graphical method for a unifying, quantitative analysis of molecular bonding-force measurements by atomic force microscopy (AFM). The method is applied to interpreting a range of phenomena commonly observed in the experimental AFM measurements of noncovalent, weak bonds between biological macromolecules. The analysis suggests an energy landscape underlying the intermolecular force and demonstrates that many observations, such as "snaps-on," "jumps-off," and hysteresis loops, are different manifestations of a double-well energy landscape. The analysis gives concrete definitions for the operationally defined "attractive" and "adhesive" forces in terms of molecular parameters. It is shown that these operationally defined quantities are usually functions of the experimental setup, such as the stiffness of the force probe and the rate of its movement. The analysis reveals a mechanical instability due to the multistate nature of molecular interactions and provides new insight into macromolecular viscosity. The graphical method can equally be applied to a quantitative analysis of multiple unfolding of subunits of the giant muscle protein titin under AFM.**

Key words: hysteresis; macromolecular viscosity; mechanical instability; nano-biochemistry; titin

INTRODUCTION

Direct measurements of noncovalent bonding force are of great importance in modern biochemistry and biophysics. Examples of noncovalent bonds range from those between proteins and their ligands to cells and their substrata. The coming of age of atomic force microscopy (AFM) and its variants provides a powerful tool for studying weak molecular interactions between cells, lipid membranes, and even between or within single macromolecules and their complexes.[1] In particular, recent novel applications of AFM in measuring bond strength within macromolecular complexes have provided a wealth of new biochemical and biomechanical information.[2–5] A quantitative and systematic analysis of these exquisite experimental data will add a new dimension to our understanding of biological processes in molecular terms. In this article, we present a unifying, yet graphical and quantitative, interpretation for these measurements. The analysis shows that many experimental observations, such as "jumps-on," "snaps-off," and hysteresis loops are manifestations of the multistate nature of molecular interactions and can all be understood in terms of an appropriate molecular energy landscape (potential of mean force) and Kramers' rate theory.[6,7] We further show that our analysis based on energy functions and the traditional analysis based on forces are conceptually equivalent, whereas each, respectively, emphasizes the chemical and mechanical aspects of molecular interactions. On the practical side, the analysis reveals the important roles played by the speed of loading and retracting the force probe (the cantilever) in an AFM measurement and the stiffness of the force probe. It demonstrates that the numerical values obtained from an AFM measurement in general depend on these parameters for conducting an experiment. Therefore, quantitative models are necessary in interpreting AFM measurements to obtain genuine biochemical quantities intrinsic to macromolecules.

Conceptually, it is important to realize that when under an external force, a macromolecule is not at its native thermal equilibrium. Therefore, molecular force measurements probe the nonequilibrium configurations of a macromolecule, which is fundamentally different from traditional equilibrium studies.[8] It is the nonequilibrium states in which many proteins and biological macromolecules perform a wide range of their functions in living processes. Therefore, it is expected, and has been demonstrated by recent quantitative analyses,[6,7,9] that the new force measurements are often kinetic in nature.

The present article is a continuation of the recent work of Shapiro and Qian[7,10] in which a stochastic analysis has been developed on the basis of the potential function of the bonding energy underlying force measurements. It has been shown that the bond rupturing (snaps-off) phenomenon commonly observed in AFM measurements is associated with a thermally activated dissociation in a double-well potential, where one energy well is identified with the molecular complex and the other with the equilibrium position of the cantilever (Fig. 1). It was also shown that in the limit of classical mechanics, i.e., in the absence of thermally activated transition, the rupture is associated with the changing of total potential energy, $E(x)$, from a

*Correspondence to: Hong Qian, Department of Applied Mathematics, University of Washington, 408 Guggenheim Hall, Seattle, WA 98195-2420.
Received 26 July 1999; Accepted 26 July 1999

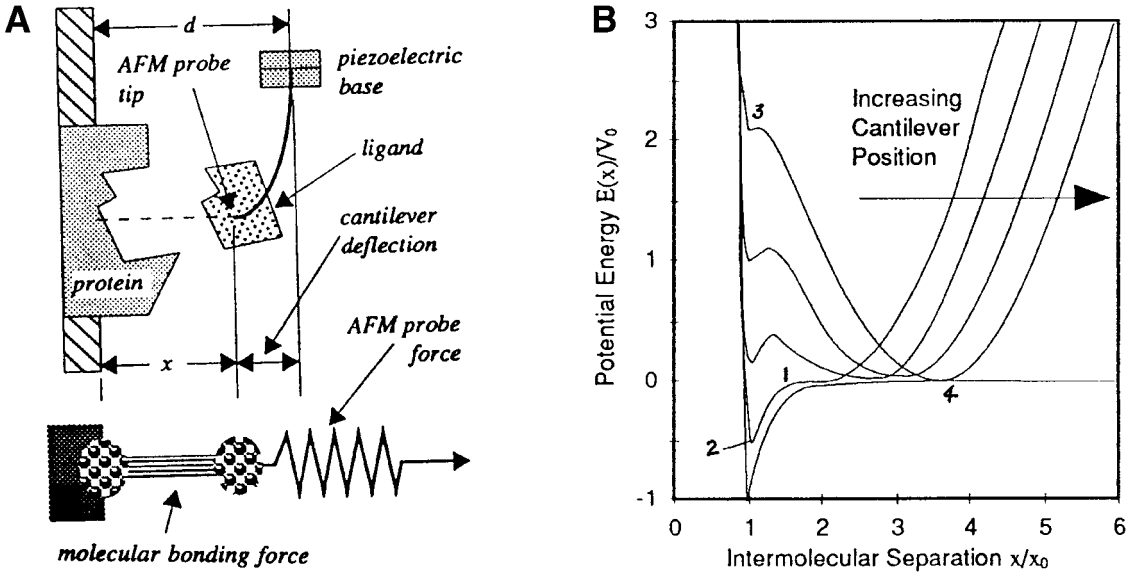

Fig. 1. **A:** Schematic for the AFM setup, where a "ligand" is attached to the tip of the AFM probe (cantilever) and a "receptor" is placed at a fixed position ($x = 0$). In a usual experiment, the base of the probe is controlled by a piezoelectric motor that moves at a regular speed. The tip of the probe is not under direct control by the experimenter; rather, its position is determined by the balance of forces between the elasticity of the probe and the interaction between the ligand and receptor. **B:** The combined total potential energy function for the ligand (Eq. 1) with various different d, the position of the base of the probe. From left to right: $d/x_0 = 2.0$, 2.5, 3.0, 3.5 with stiffness of the probe being $kx_0^2/V_0 = 1$. x_0 and V_0 are the parameters in a 6–12 potential for noncovalent intermolecular bonding:

$$U(x) = -V_0[2(x_0/x)^6 - (x_0/x)^{12}]$$

The labels 1, 2, 3, and 4 correspond to these in Figure 3. The right energy well becomes lower than the left one when d/x_0 is somewhere between 2.0 and 2.5. [Adapted from Shapiro and Qian[7] with permission from Elsevier Science.]

double-well to a single-well due to the movement of the piezoelectric motor that drives the cantilever. A graphical method based on the force diagram corresponding to the potential energy analysis that intuitively illustrates the physics of a pulling process for protein-ligand separation has been developed. The graphical method obviates the cumbersome mathematical derivations required for the analysis[10] and is accessible to all biochemical researchers.

In this article, we apply the same graphical method to analyze yet another commonly observed phenomenon in AFM measurements: a hysteresis loop. There are two components of the hysteresis. One relates to a separation between the loading and retraction curves after the "jumps-on." The other relates to a difference in x positions when the jumps-on and snaps-off occur. It is shown that all these components are associated with the presence of two occasions at which the intermolecular force gradient equals the negative spring constant of the probe. Furthermore, based on the present analysis, quantitative definitions for operationally defined *attractive force* and *adhesive force*[11,12] are obtained. To illustrate our analysis in a concrete fashion, we use the 6–12 spoon-shaped (Lennard-Jones) potential and refer the moving component attached to the tip of the cantilever as ligand and the fixed component as receptor. Use of the particular potential is not meant to be realistic, but merely to serve as an example. The principle of the graphical method is applicable to any realistic potential function. Finally, we also apply the graphical method to a multiple-rupture process using the multiple unfolding of subunits of the giant muscle protein titin as an example.

GRAPHICAL METHOD FOR FORCE ANALYSIS

Figure 1 encompasses the basic assumption of our analysis. We assume that the cantilever is a Hookean element with spring constant k. The total force on the ligand is the sum of the molecular bonding force due to the interaction with receptor and the force from the cantilever. When these two forces are balanced, the force on the cantilever constitutes a measurement for the bonding force. Figure 1B shows the combined total potential energy for the ligand[7]:

$$E(x) = U(x) + \frac{k}{2}(x - d)^2 \qquad (1)$$

where d is the position of the piezoelectric motor (Fig. 1A).

The most eminent feature of the total potential function $E(x)$ is the presence of two energy wells, with a barrier in between, for a wide range of k and d (Fig. 1). This corresponds to a nonmonotonic force curve; hence, there is a region of negative spring constant. The forces on the ligand are zero when it is at either an energy minimum or maximum. Figure 2A shows these zero force positions (i.e., equilibrium positions) as functions of d and k. It is seen that when the base is retracted from the receptor (increasing d), the energy function switches from having one single well to having two wells, and back to a single well again when d is very large. Figure 2B shows the regions for parameters k and d in which the system has single and double wells.

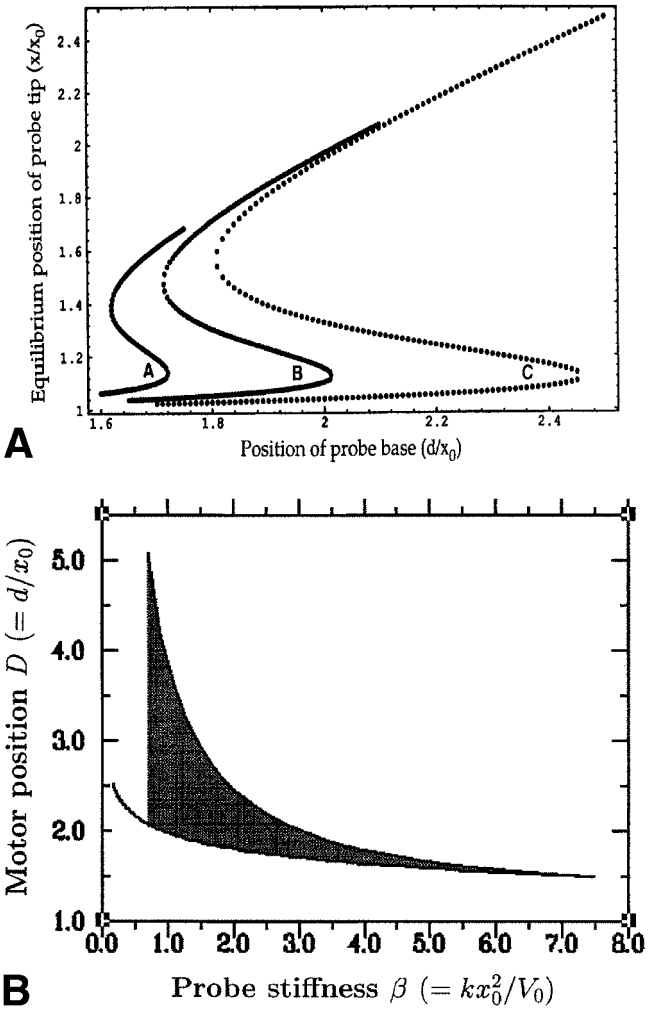

Fig. 2. **A:** The equilibrium (zero force) position of the ligand as function of the motor position (d) for various stiffness of the probe (k). These equilibrium positions are defined as the extreme of the total potential energy function $E(x)$ (Eqs. 1 and 3). Curves A, B, and C correspond to different probes with stiffness $kx_0^2/V_0 = 4.5$, 3.0, and 2.0. In the regions that have multiple equilibria, there are two energy minima with an energy barrier in between. These are the regions where thermal activated stochastic dissociation occur. The regions with negative slopes reflect the ''blind'' regions that cannot be accessed by experimental measurements. Increasing stiffness decreases the blind region. **B:** Different regions for the parameters of the force probe: stiffness $\beta = kx_0^2/V_0$ and motor position $D = d/x_0$. Upper-right region: Single well associated with the force probe. Lower-left region: single well associated with the molecular bond. Shadowed region: two wells where the ligand-protein dynamics is thermally activated. The equations for the curves are given parametrically

$$\beta = 12[7u^{-8} - 13u^{-14}] \text{ and } D = (8u^7 - 14u)/(7u^6 - 13).$$

Note the maximal stiffness is when $\beta = 7.48$ beyond which the stochastic region no longer exists.

Graphical Interpretation of Hysteresis Loop

The graphical method of analyzing force is illustrated in Figure 3. A force measurement is made when the total potential energy function $E(x)$ is at its minimum, when the bonding force is balanced by the harmonic spring of the AFM:

$$\frac{dE(x)}{dx} = \frac{dU(x)}{dx} + k(x - d) = 0. \tag{2}$$

In Figure 3, we plot the force as a function of x, $F_{bond}(x) = dU(x)/dx$, for the molecular potential function $U(x)$ (solid curve). In the same plot, the force for the harmonic spring is a straight line with slope $-k$ and abscissa intercept d. Thus, the force measurement from the AFM at each x is easily obtained if we locate the intersection(s) between the $F_{bond}(x)$ and the line $-k(x - d)$.

When the ligand is approaching the receptor at $x = 0$, the parallel line moves leftward with decreasing d. It should be noted, however, that between the two solid lines AB and CD, there are three intersections rather than one (Fig. 3). These correspond to the two minima and the intervening barrier in the total energy function $E(x)$. This is the regimen where thermally activated transitions occur at finite temperature.[7] In the limit of extreme low temperature, one can neglect the thermal transition. Thus, when the tip (ligand) is approaching the receptor, it follows the highlighted curve (and arrows) shown in Figure 3, starting at the far right. When the tip (ligand) is at point 1, it is pulled toward the receptor, exhibiting a *snap:* an irreversible process in which energy is lost because of viscous damping. (Note that even though viscous damping is not explicitly included in our analysis, the energy dissipation due to the snap is necessary because the ligand moves in an aqueous solution.) This is when the energy barrier disappears, and the energy well at point 1 becomes unstable, being taken over by the energy minimum at point 2. During retraction, the tip will again follow the highlighted line from far left, passing point 3 and the peak of the force curve. When it is at point 3, the bond ruptures and the tip jumps back to point 4. So the complete path of $4 \rightarrow 1 \rightarrow 2 \rightarrow 3 \rightarrow 4$ forms a hysteresis loop.

Although the above analysis regards only low temperature limits, the hysteresis associated with the jumps-on and snaps-off would still be expected at a finite temperature in the form of cooperative thermal transition. The appearance of the hysteresis loop, however, is usually stochastic.

Attractive and Adhesive Forces

Figure 3 shows that the adhesive force, although varying with the value of the cantilever stiffness k, approximately equals the maximum of the bonding force. However, the attractive force varies with the value of k to a much larger extent (Fig. 4). The attractive force is always less than adhesive force.[11] If the cantilever spring is sufficiently stiff ($k > 7.48V_0/x_0^2$), i.e., greater than the maximal negative force gradient, then there will be no hysteresis. Thus, hysteresis is another manifestation of the kinetic nature of the AFM measurements on weak (soft) interaction. The portion of the force curve between 1 and 3 has been called a *blind region* because it is not

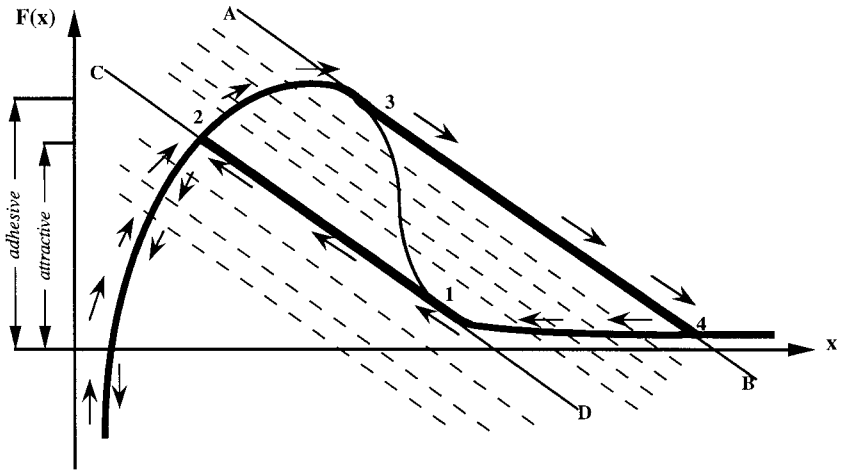

Fig. 3. Schematic illustration for the graphical method of determining the equilibrium position and measured force by AFM. Closed curve 41234 forms a hysteresis loop.

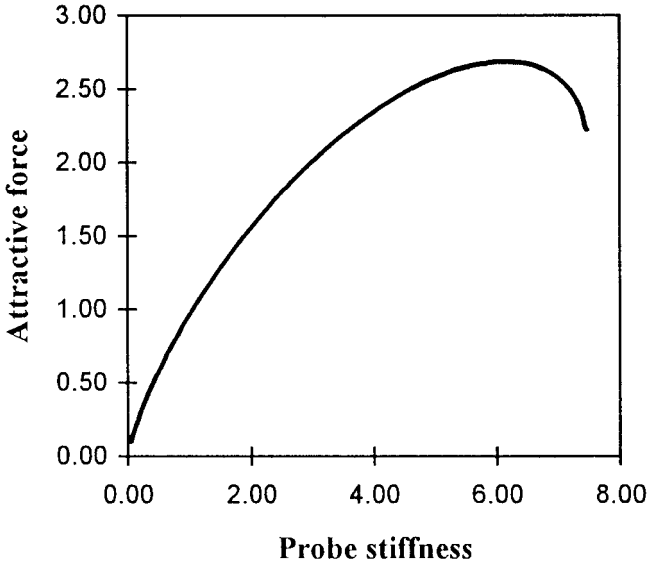

Fig. 4. The attractive force as a function of the stiffness of the AFM probe. In this calculation we have assumed the 6–12 (Lennard-Jones) bonding force (Eq. 3). The units for abscissa (k) and ordinate ($F_{attractive}$) are V_0/x_0^2 and V_0/x_0, respectively. The attractive force is always less than the adhesive force (i.e., the peak value of the curve) and equals the adhesive force when the probe is sufficiently stiff. The blind region disappears all together when k is $>7.48V_0/x_0^2$, that is, when the probe is stiffer than any part of the bonding force curve.

experimentally accessible by AFM with the particular k.[7] The greater the stiffness k, the smaller the blind region.

Figure 3 shows that the line segments $\overline{12}$ and $\overline{34}$ of the force-displacement curve (the highlighted curve) are parallel, because they both follow the probe stiffness with its base position fixed. Here we have assumed that both the jumps-on and snaps-off are instantaneous. If, however, the snap has a speed comparable with that of the advancing piezoelectric motor, then the force will be kept almost constant during loading, i.e., the slope of the line segment $\overline{12}$ could be almost zero. This indeed has been observed.[11] Similarly, one expects the slope for line segment $\overline{34}$ to be less than that shown in Figure 3. In our analysis, we have also neglected the effect of viscous drag, or more generally, the viscoelastic nature of bonding force.[13] Including this effect will lead to a further separation between the loading and retraction paths with even larger hysteresis.[4] According to our analysis, the difference between the attractive and adhesive forces has the same molecular origin as the snaps-on and jumps-off. In more complex systems, however, the adhesive hysteresis is a more complex issue that requires further investigation.

Subunit Unfolding of Titin by AFM

The graphical method can also be applied to the experiments in which multiple ruptures are observed. Let's consider the recent force measurements on protein titin.[14–16] We will focus on analyzing the sawtooth behavior[14]; a more comprehensive analysis will be published elsewhere. The sawtooth behavior can be analyzed with the following two assumptions: (a) A single globular subunit can be in either folded or unfolded states, and it unfolds under an external force F^*. The situation is analogous to the protein-ligand dissociation under external force. (b) The folded state is completely rigid without any elasticity, and the unfolded state is a wormlike polymer chain with characteristic force-extension: $F(x) = (k_BT/l)[x/L + 1/4(1 - x/L)^2 - 1/4]$ where l and L are persistence and total length of the polymer chain of a single subunit.[15] With thermal activation a subunit can unfold, with finite probability, even under a force much smaller than F^*,[7] or no force at all.[17]

The sawtooth behavior is demonstrated in Figure 5. We assume that there are totally N identical subunits. If one pulls a molecule with n unfolded and $N - n$ folded subunits, its force-extension relation should be $F(x/n)$. This follows directly from the equilibrium law for serial springs. The curves in Figure 5 (A–D) are for $n = 3$ to $n = 6$ unfolded subunits, respectively. When pulling a titin with three unfolded subunits, the force follows the curve A and is built up until it reaches F^*, and then an additional domain unfolds, and now the force should follow curve B. As in the case of protein-ligand separation, the rupture follows a straight line determined be the probe stiffness of

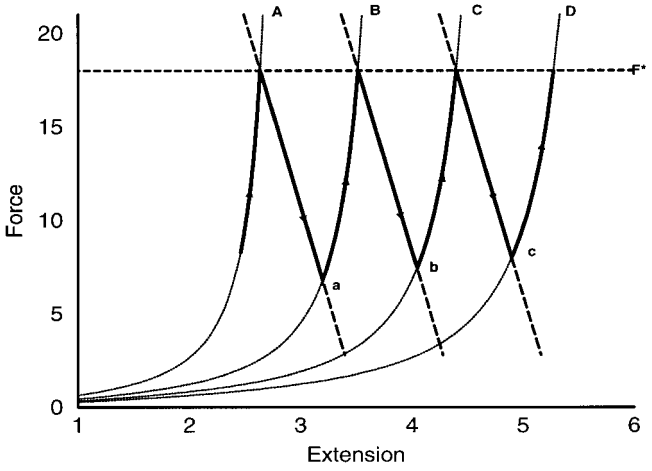

Fig. 5. Schematic illustration for the multiple unfolding of subunits of titin. The extension (abscissa) is in units L. The force (ordinate) is in units k_BT/l. The dotted lines are force-extension relation for n unfolded subunits in serial: $x/n + 1/4(1 - x/n)^2 - 1/4$ with $n = 3, 4, 5, 6$ (A–D). The dashed lines have slope $-k$ representing the spring constant of the cantilever. When the force reaches F^*, a subunit will unfold, similar to the "snaps-off" in Figure 3. The forces at troughs are shown to increase from a to b to c.

AFM. This process repeats. The troughs of curve a, b, c, etc. can be quantitatively determined from the equation: $F(x/n) = -k[x - (n - 1)x^*] + F^*$ where x^* is strain at which an individual subunit unfold: $F^* = F(x^*)$. For stiff cantilever, i.e., large k, solution of this equation shows that the forces at troughs increase with n, as observed experimentally.

The experimental measurements, however, show also an increasing peak force. One simple explanation is that not all the subunits are perfectly identical. In this case, both peaks and troughs increase. Alternatively, if there is significant thermal activation, then the rate of thermally activated unfolding is greater at earlier stage (smaller n) because more subunits (i.e., $N - n$) are available to be unfolded. Therefore, less force is needed, stochastically speaking, to unfold a domain for smaller n. Hence, the peak is lower for the smaller n. (HQ thanks Dr. William Hancock for an insightful discussion on this point).

DISCUSSION

Direct measurements of the noncovalent bonding forces between and within macromolecules and macromolecular complexes have opened a new chapter in biophysics and physical biochemistry. Until recently there has been almost no systematic method for experimentally performing such measurements. Notable exceptions are the pioneering work on cellular mechanics by micropipette aspiration[18] and cell poking.[13,19,20] In this article, we have shown how the traditional force analysis can be interpreted in terms of an energy landscape (potential of mean force), thus providing a bridge between mechanics and thermodynamics of macromolecules.

Stiffness and Speed of AFM Probe

Our analysis has clearly demonstrated the importance of the stiffness of AFM probes in a quantitative measurement of molecular bonding force. The choice of the stiffness in the laboratory is a compromise between the needs for the range and the accuracy of the measurement. A stiff probe can provide a wider measurement range with a smaller blind region, but it lowers the accuracy of the force measurements that are based on the deflection of the probe: there is a relatively larger experimental error in measuring a smaller deflection. The accuracy, however, can often be improved by increasing the sophistication in measuring small deflection. From a data interpretation point of view, the difficulty in analyzing the force-displacement relationship from a soft probe is that neither the probe force nor the tip displacement is under the control of the experimenter. This is in sharp contrast to the conventional mechanical measurements in terms of relaxation and creep functions,[21] in which either the force or the displacement is precisely controlled. As a consequence, the velocity of the probe tip is a variable in the measurement, and the instantaneous force-displacement relationship is often compounded with the effect of viscosity. One could minimize the viscosity effect by slow loading and pulling. However, slow processes lead to significant thermally activated stochastic barrier crossing, which invalidates a simple mechanical interpretation.[7]

Characterization of Molecular Bonding Potential by AFM

Figure 3 also shows the relevant information one obtains from the indentation and the pulling parts of the ramp, respectively. Both give the zero force region. Specifically, both yield the position and the curvature of the harmonic energy well of the bonding potential. Note the main information about the thermodynamics of the molecular bonding is from this region. The maximal (adhesive) force obtained by a pulling measurement corresponds to the region where the energy function significantly deviates from the harmonicity; this region is more relevant to the kinetics of the dissociation of the molecular complex. The region between the jumps-on and snaps-off points is the blind region where the molecular force has a stiffer negative spring than the probe. A complete potential energy function, therefore, can be reasonably reconstructed by a piecewise merge of (a) a hard wall and an energy well, (b) the inflection point corresponding to the maximal force, (c) a cubic curve with curvature $-k$ at the jumps-on and snaps-off points, representing the blind region, and (d) an exponential decay connecting the jumps-on point to the infinity.

Chemical Versus Mechanical Views of Macromolecular Viscosity

Hysteresis is also observed in the force measurements on polymer gels by cell poking.[13,18,19] It is well known that macromolecular structures and their slow relaxation are responsible for the macroscopic viscosity of polymer solutions (the chemical view, Qian et al.[22]). The slow relaxation is, of course, a consequence of energy barrier crossing on the molecular level. The type of hysteresis we encounter in the present work, therefore, is the ultimate origin of

macroscopic viscosity of polymer solution. Mechanical instability, when occurring in viscous solvent, leads to large energy dissipation. This is the mechanical view of the macromolecular viscosity.

Two Aspects of Macromolecular Mechanics

AFM studies of macromolecules and macromolecular complex provide a rich amount of information on the mechanics of macromolecules. There are two different point of views on the subject. Biophysicists are interested in the force involved in molecular events,[23] and physical biochemists are interested in the free energy of the molecular complex.[24] Because a force can only be generated in a nonequilibrium state,[25,26] it is natural that many interesting biophysical processes involve the peak region of the force curve, i.e., the kinetics. However, for the thermodynamicists the zero force region is more relevant. At a given external force, a molecule reaches a new equilibrium state that corresponds to a nonequilibrium state of the molecule with low probability in the absence of the force. Therefore, studying macromolecules under force is an experimental realization of the umbrella sampling commonly used in computational biochemistry.[27,28]

Future Research in Macromolecular Mechanics

The major assumption behind our above analysis is the neglect of internal structures and dynamics of the macromolecules. It can be shown that this assumption is valid if the internal conformational dynamics is fast with respect to the AFM measurements. We shall call this assumption rapid internal dynamics (RID) hypothesis. For macromolecules in which the RID does not hold, the external force will also influence the conformational dynamics of the molecule, and a higher dimensional characterization of the molecular system with internal coordinates is necessary. One particular interesting example is the mechanics of titin which exhibits a wide range of interesting mechanical behavior[15,16] in addition to the sawtooth behavior we discussed.[14] Treating the internal conformations and external forces on an equal footing is the future of macromolecular mechanics.

ACKNOWLEDGMENTS

We thank Professors Carlos Bustamante, Joe Howard, Buddy Ratner, and Pedro Verdugo for discussion and encouragement. HQ thanks Bill Daily and Elliot Elson for those long discussions between 1983 and 1984 on hysteresis on cell-poking experiments that left an everlasting impression on force measurements.

REFERENCES

1. Fernandez JM. Cellular and molecular mechanics by atomic force microscopy: capturing the exocytotic fusion pore in vivo? Proc Natl Acad Sci USA 1997;94:9–10.
2. Florin EL, Moy VT, Gaub HE. Adhesion forces between individual ligand-receptor pairs. Science 1994;264:415–417.
3. Lee GU, Chrisey LA, Colton RJ. Direct measurement of the force between complementary strands of DNA. Science 1994;266:771–773.
4. Boland T, Ratner BD. Direct measurement of hydrogen bonding in DNA nucleotide bases by atomic force microscopy. Proc Natl Acad Sci USA 1995;92:5297–5301.
5. Evans E, Ritchie K, Merkel R. Sensitive force technique to probe molecular adhesion and structural linkages at biological interfaces. Biophys J 1995;68:2580–2587.
6. Evans E, Ritchie K. Dynamic strength of molecular adhesion bonds. Biophys J 1997;72:1541–1555.
7. Shapiro BE, Qian H. A quantitative analysis of single protein-ligand complex separation with the atomic force microscope. Biophys Chem 1997;67:211–219.
8. Tanford C. Physical chemistry of macromolecules. New York: Wiley & Sons; 1961.
9. Chilkoti A, Boland T, Ratner BD, Stayton PS. The relationship between ligand-binding thermodynamics and protein-ligand interaction forces measured by atomic force microscopy. Biophys J 1995;69:2125–2130.
10. Shapiro BE, Qian H. Hysteresis in force probe measurements: a dynamic systems perspective. J Theor Biol 1998;194:551–559.
11. Burnham NA, Dominguez DD, Mowery RL, Colton RJ. Probing the surface forces of monolayer filmes with an atomic-force microscope. Phys Rev Lett 1990;64:1931–1934.
12. Burnham NA, Colton RJ. Measuring the nanomechanical properties and surface forces of materials using a atomic force microscope. J Vac Sci Tech A 1989;7:2906–2913.
13. Zahalak GI, McConnaughey WB, Elson EL. Determination of cellular mechanical properties by cell poking, with an application to leukocytes. J Biomech Engng 1990;112:283–294.
14. Rief M, Gautel H, Oesterhelt F, Fernandez JM, Gaub HE. Reversible unfolding of individual titin immunoglobulin domains by AFM. Science 1997;276:1109–1112.
15. Kellermayer MSZ, Smith SB, Granzier HL, Bustamante C. Folding-unfolding transitions in single titin molecules characterized with laser tweezers. Science 1997;276:1112–1116.
16. Tskhovrebova L, Trinick J, Sleep JA, Simmons RM. Elasticity and unfolding of single molecules of the giant muscle protein titin. Nature 1997;387:308–312.
17. Qian H, Chan SI. Hydrogen exchange kinetics of proteins in denaturants: a generalized two-process model. J Mol Biol 1999;286: 607–616.
18. Evans E, Hochmuth RM. Mechanochemical properties of membranes. Curr Top Membr Transp 1978;10:1–64.
19. Petersen NO, McConnaughey WB, Elson EL. Dependence of locally measured cellular deformability on position on the cell, temperature, and cytochalasin B. Proc Natl Acad Sci USA 1982;79: 5327–5331.
20. Duszyk M, Schwab B, Zahalak GI, Qian H, Elson EL. Cell poking: quantitative analysis of indentation of thick viscoelastic layers. Biophys J 1989;55:683–690.
21. Fung YC. Foundations of solid mechanics. Englewood Cliffs, NJ: Prentice-Hall; 1995.
22. Qian H, Elson EL, Frieden C. Studies of the structure of actin gels using time correlation spectroscopy of fluorescence beads. Biophys J 1992;63:1000–1010.
23. Svoboda K, Block SM. Biological applications of optical forces. Annu Rev Biophys Biomol Struct 1994;23:247–285.
24. Jorgensen WL. Free energy calculations: a breakthrough for modeling organic chemistry in solution. Acc Chem Res 1989;22: 184–189.
25. Qian H. A simple theory of motor protein kinetics and energetics. Biophys Chem 1997;67:263–267.
26. Qian H. Vector field formalism and analysis for a class of thermal ratchets. Phys Rev Lett 1998;81:3063–3066.
27. Chandler, D. Introduction to modern statistical mechanics. New York: Oxford University Press; 1987.
28. Izrailev S, Stepaniants S, Balsera M, Oono Y, Schulten K. Molecular dynamics study of unbinding of the avidin-biotin complex. Proteins 1997;72:1568–1581.